

Fundamental Aspects of Droplet Combustion Modelling

Shah Shahood Alam*, Ahtisham A. Nizami, Tariq Aziz

*Corresponding author. Address: Pollution and Combustion Engineering Lab. Department of Mechanical Engineering, Aligarh Muslim University, Aligarh-202002, U.P. India.

ABSTRACT

The present paper deals with important aspects of liquid droplet evaporation and combustion. A detailed spherically symmetric, single component droplet combustion model is evolved first by solving time dependent energy and species conservation equations in the gas phase using finite difference technique. Results indicate that the flame diameter F first increases and then decreases and the square of droplet diameter decreases linearly with time. Also, the F/D ratio increases throughout the droplet burning period unlike the quasi-steady model where it assumes a large constant value. The spherically symmetric model is then extended to include the effects of forced convection. Plots of D^2 and droplet mass burning rate m_f versus time are obtained for steady state, droplet heating and heating with convection cases for a n-octane droplet of 1.3 mm diameter burning in standard atmosphere. It is observed that the mass burning rate is highest for forced convective case and lowest for droplet heating case. The corresponding values of droplet lifetime follow the inverse relationship with the mass burning rate as expected. Emission data for a spherically symmetric, 100 μm n-heptane droplet burning in air are determined using the present gas phase model in conjunction with the Olikara and Borman code [1] with the aim of providing a qualitative trend rather than quantitative with a simplified approach. It is observed that the products of combustion maximise in the reaction zone and NO concentration is very sensitive to the flame temperature. This paper also discusses the general methodology and basic governing equations for analysing multicomponent and high pressure droplet vaporisation/combustion in a comprehensible manner. The results of the present study compare fairly well with the experimental/theoretical observations of other authors for the same conditions. The droplet sub models developed in the present work are accurate and yet simple for their incorporation in spray combustion codes.

Keywords: droplet combustion models, gas and liquid phases, numerical solution, simplified approach, spray combustion codes.

I. Introduction

Combustion of liquid fuels provide a major portion of world energy supply. In most of the practical combustion devices like diesel engines, gas turbines, industrial boilers and furnaces, liquid rockets, liquid fuel is mixed with the oxidiser and burned in the form of liquid sprays (made up of discrete droplets). A spray may be regarded as a turbulent, chemically reacting, multicomponent (MC) flow with phase change involving thermodynamics, heat and mass transport, chemical kinetics and fluid dynamics.

Further, the submillimeter scales associated with spray problem have made detailed experimental measurements quite difficult. Hence in general, theory and computations have led experiments in analysing spray systems [2] with the aim to establish design criteria for efficient combustors from combustion and emission point of view.

Since direct studies on spray combustion may be tedious and inaccurate, an essential pre-requisite for understanding spray phenomenon is the knowledge of the laws governing droplet evaporation and

combustion with the main objective of developing computer models to give a better understanding of spray combustion phenomenon. However, the droplet models should be realistic and not too complicated, so that they can be successfully employed in spray codes, where CPU economy plays a vital role [2].

An isolated droplet combustion under microgravity (near zero gravity) condition is an ideal situation for studying liquid droplet combustion phenomenon. It leads to a simplified, one dimensional solution approach of the droplet combustion problem.

The resulting model is called 'spherico-symmetric droplet combustion model' (a spherical liquid fuel droplet surrounded by a concentric, spherically symmetric flame, with no relative velocity between the droplet surface and surrounding gas, that is, gas phase Reynolds number based on droplet diameter $Re_g = 0$).

Droplet combustion models available in the literature are of varied nature. Most simplified

models assume quasi-steadiness in both liquid droplet and the surrounding gas phase.

In the quasi-steady liquid phase model, the liquid droplet is at its boiling point temperature evaporating steadily with a fixed diameter surrounded by a concentric stationary flame, such that the F/D ratio, also known as flame standoff ratio assumes a constant value.

The justification of this assumption is based on the relatively slow regression rate of the liquid fuel droplet as compared to gas phase transport processes.

For the combustion of single component liquid droplets or light distillate fuel oils in high temperature ambient gas atmosphere, it is quite accurate to assume that the droplet is at its boiling point temperature $T_s = T_b$ [3], (i.e. no droplet heating or no need for solving the unsteady energy equation within the liquid phase). The droplet evaporates steadily following the d^2 -law (square of instantaneous droplet diameter varying linearly with time).

This quasi-steady liquid phase can be coupled with a steady or unsteady gas phase. It is more realistic to adopt a non-steady gas phase since the flame front is always moving as suggested by the experiments [4,5]. The gas phase analysis requires the solution of unsteady energy and species conservation equations (partial differential equations).

In practical applications, droplets in a spray will be moving at some relative velocity to the surroundings. The Reynolds number based on relative velocity and gas properties can be of the order of 100 [2]. Boundary layer present due to convection, surrounding the droplet enhances heat and mass transport rates over the values for the spherically symmetric droplet. Further, shear force on the liquid surface causes an internal circulation that enhances the heating of the liquid. As a result,

vaporisation rate increases with increasing Reynolds number.

The general approach adopted in dealing with droplet vaporisation/combustion in forced convective situations has been to model the drop as a spherically symmetric flow field and then correct the results with an empirical correlation for convection [2,6].

For the fast oxidation case, it is not generally necessary to analyse the structure of the thin flame surrounding the droplet in order to predict the vaporization rate. The structure of flames are however relevant for the prediction and understanding of pollutant formation.

An important aspect which is currently under experimental and theoretical investigation is multicomponent droplet combustion. The commercial fuels used in engines are multicomponent in nature, where different components vaporise at different rates. Here the analysis of liquid phase becomes important and the droplet combustion model may assume a fully transient approach (unsteady liquid and gas phases).

High pressure/supercritical combustion phenomenon occurring in gas turbines, diesel and rocket engines is another recent issue related to droplet combustion where manufacturers are looking for improved engine efficiency and power density. Some studies have indicated that in these situations d^2 -law is still followed while some have shown it is not. Apart from this, there are other important considerations like representation of high pressure liquid-vapour equilibrium for each component, solubility of ambient gas into the liquid and determination of pressure dependent thermophysical and transport properties.

In the present paper, we shall first investigate in detail, the spherically symmetric, single component droplet combustion model obeying the

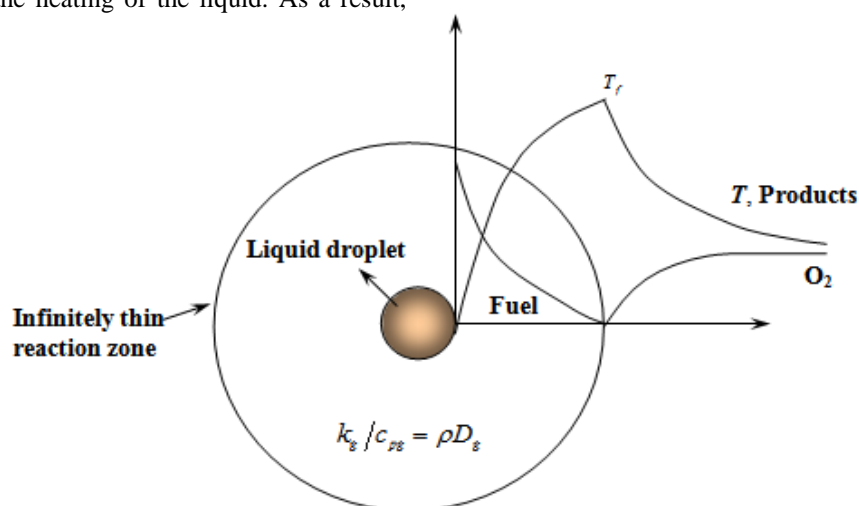


Fig. 1(a) Classical d^2 -law model (Godsave and Spalding, early 1950s)

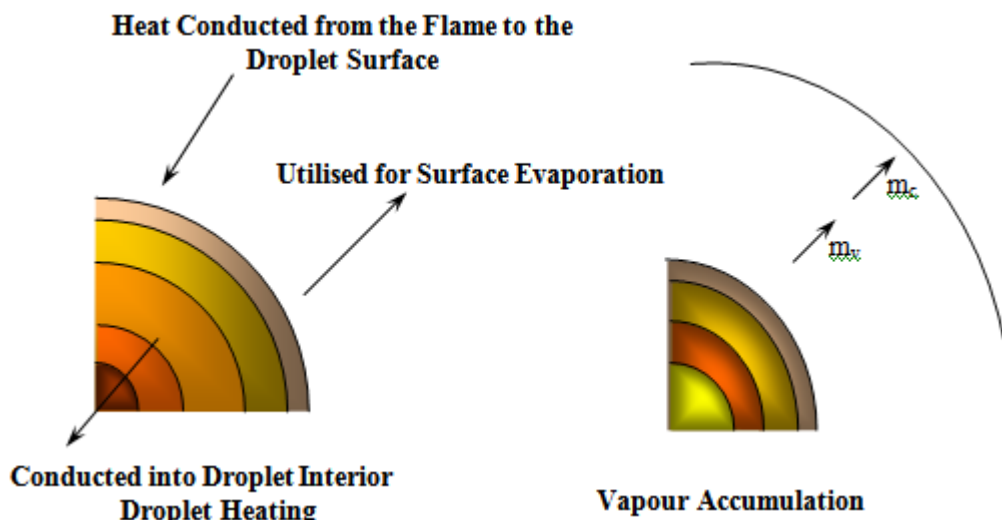


Fig. 1(b) Relaxation of d^2 -law assumption (Law, 1976 and 1980)

d^2 -law, coupled with an unsteady gas phase. This model shall be extended to include convective effects. After that, a general variation of species concentration profiles or emission characteristics which include CO, CO₂, H₂O and NO around a burning fuel droplet shall be obtained using the unsteady gas phase model described above.

The basic essentials of liquid phase analysis which are fundamental for developing a realistic multicomponent droplet evaporation/combustion model will be taken up next. Finally, we shall be discussing in brief the important equations and methodology for developing a high pressure droplet vaporisation model.

We start with a brief literature review of the above mentioned droplet sub models.

Kumagai and co-workers [5,7,8] were pioneers in conducting spherically symmetric droplet combustion experiments in microgravity conditions through drop towers, capturing the flame movement and further showed that F/D ratio varies throughout the droplet burning history.

Waldman [9] and Ulzama and Specht [10] used analytical procedure whereas Puri and Libby [11] and King [12] employed numerical techniques in developing spherically symmetric droplet combustion models. The results of these authors were mainly confined to the observations that unlike quasi-steady case, flame is not stationary and flame to droplet diameter ratio increases throughout the droplet burning period.

A study on convection was carried out by Yang and Wong [13] who investigated the effect of heat conduction through the support fibre on a droplet vaporising in a weak convective field. Another aspect related to convection is the presence of internal circulation within the droplet. Law, C.K [14] introduced the 'infinite diffusivity' or 'batch distillation' model which assumed internal

circulation within the droplet. Droplet temperature and concentrations were assumed spatially uniform but temporally varying. It was suggested that the more volatile substance will vaporise from the droplet surface leaving only the less volatile material to vaporise slowly.

In the absence of internal circulation, the infinite diffusivity model was found to be inappropriate. For such conditions Landis and Mills [15] carried out numerical analysis to solve the coupled heat and mass transfer problem for a vaporising spherically symmetric, miscible bicomponent droplet. This model in literature is termed as 'diffusion limit' model.

Law, C.K [16] generalised the formulation of Landis and Mills and suggested that regressing droplet surface problems are only amenable to numerical solutions. Tong and Sirignano [17] devised a simplified vortex model which required less computing time than the more detailed model of Lara-Urbaneja and Sirignano [18].

In an experimental investigation, Aldred et al. [19] used the steady state burning of n-heptane wetted ceramic spheres for measuring the flame structure and composition profiles for the flame corresponding to 9.2mm diameter sphere. Their results indicated that oxidizer from the ambient atmosphere and fuel vapour from the droplet surface diffuse towards each other to form the flame where the products of combustion are formed and the flame temperature is highest.

Marchese and Dryer [20] considered detailed chemical kinetic modelling for the time dependent burning of isolated, spherically symmetric liquid droplets of methanol and water using a finite element chemically reacting flow model. It was noted that a favourable comparison occurred with microgravity droplet tower experiment if internal liquid circulation was included which could be caused by droplet

generation/deployment techniques. However, significant deviations from the quasi-steady $d^2 - law$ were observed.

As mentioned before, the recent trend in the utilisation of synthetic and derived fuels has generated renewed interest in the vaporisation and combustion of multicomponent liquid fuel droplets. The fuel vaporization process is crucial in determining the bulk combustion characteristics of multicomponent fuel spray and its influence on pollution formation.

For analysing multicomponent droplet vaporisation/combustion model, the liquid droplet will not be assumed to be at its boiling point temperature and therefore the problem becomes involved, since one has to solve the time dependent energy equation in the liquid phase in addition to the transient liquid phase species mass diffusion equation.

Law and Law [21] formulated a $d^2 - law$ model for a spherically symmetric, multicomponent droplet vaporisation and combustion. It was noted that the mass flux fraction or the fractional vaporisation rate ε_m was proportional to the initial liquid phase mass fraction of that species prior to vaporisation. The simplified vortex model of Tong and Sirignano [17] was another valuable contribution in the analysis of multicomponent droplet evaporation.

Apart from that, the modelling results of Shaw [22] suggested that $d^2 - law$ is followed after the decay of initial transients for the case of spherical combustion of miscible bicomponent droplets. A comprehensive experimental investigation was conducted by Sorbo et al. [23] to quantify the combustion characteristics of pure CHC_s (chlorinated hydrocarbons) as well as their mixtures with regular hydrocarbon fuels for enhancing the incinerability of CHC_s .

Some important contributions to high pressure droplet evaporation and combustion are provided by the following researchers.

Chin and Lefebvre [3] investigated the effects of ambient pressure and temperature on steady state combustion of commercial multicomponent fuels like aviation gasoline, JP5 and diesel oil (DF2). Their results suggested that evaporation constant values were enhanced as ambient pressure and temperature were increased.

Kadota and Hiroyasu [24] conducted an experimental study of single suspended alkanes and light oil droplets under natural convection in supercritical gaseous environment at room temperatures. It was noted that combustion lifetime decreased steeply with an increase in reduced pressure till the critical point whereas burning

constant showed a continuously increasing trend with reduced pressure in both sub and supercritical regimes.

Deplanque and Sirignano [25] developed an elaborate numerical model to investigate spherically symmetric, transient vaporisation of a liquid oxygen (LOX) droplet in supercritical gaseous hydrogen. They advocated the use of Redlich-Kwong equation of state (EOS) and suggested it can be assumed that dissolved hydrogen remains confined in a thin layer at the droplet surface. Further it was observed that vaporisation process followed the $d^2 - law$.

Zhu and Aggarwal [26] carried out numerical investigation of supercritical vaporisation phenomena for n-heptane- N_2 system by considering transient, spherically symmetric conservation equations for both gas and liquid phases, pressure dependent thermophysical properties and detailed treatment of liquid-vapour phase equilibrium employing different equations of state.

II. Problem Formulation

2.1 Development of spherically symmetric droplet combustion model for the gas phase

As mentioned before, droplet combustion experiments have shown that liquid droplet burning is a transient phenomenon. This is verified by the fact that the flame diameter first increases and then decreases and flame to droplet diameter ratio increases throughout the droplet burning unlike the simplified analyses where this ratio assumes a large constant value. Keeping this in mind, an unsteady, spherically symmetric, single component, diffusion controlled gas phase droplet combustion model is developed by solving the transient diffusive equations of species and energy.

Important assumptions invoked in the development of spherically symmetric gas phase droplet combustion model of the present study

Spherical liquid fuel droplet is made up of single chemical species and is assumed to be at its boiling point temperature surrounded by a spherically symmetric flame, in a quiescent, infinite oxidising medium with phase equilibrium at the liquid-vapour interface expressed by the Clausius-Clapeyron equation.

Droplet processes are diffusion controlled (ordinary diffusion is considered, thermal and pressure diffusion effects are neglected). Fuel and oxidiser react instantaneously in stoichiometric proportions at the flame. Chemical kinetics is infinitely fast resulting in flame being represented as an infinitesimally thin sheet.

Ambient pressure is subcritical and uniform. Conduction is the only mode of heat transport, radiation heat transfer is neglected. Soret and Dufour effects are absent.

Thermo physical and transport properties are evaluated as a function of pressure, temperature and composition. Ideal gas behaviour is assumed. Enthalpy ‘ h ’ is a function of temperature only. The product of density and diffusivity is taken as constant. Gas phase Lewis number Le_g is assumed as unity.

The overall mass conservation and species conservation equations are given respectively as:

$$\frac{\partial \rho}{\partial t} + \frac{1}{r^2} \frac{\partial}{\partial r} (r^2 \rho v_r) = 0 \quad (1)$$

$$\frac{\partial (\rho Y)}{\partial t} + \frac{1}{r^2} \frac{\partial}{\partial r} r^2 \left[\rho v_r Y - \rho D \frac{\partial Y}{\partial r} \right] = 0 \quad (2)$$

Where;

t is the instantaneous time

r is the radial distance from the droplet center

ρ is the density

v_r is the radial velocity of the fuel vapour

D is the mass diffusivity

Y is the mass fraction of the species

equations (1) and (2) are combined to give species concentration or species diffusion equation for the gas phase as follows

$$\frac{\partial Y}{\partial t} = D_g \frac{\partial^2 Y}{\partial r^2} + \frac{2D_g}{r} \frac{\partial Y}{\partial r} - v_r \left(\frac{\partial Y}{\partial r} \right) \quad (3)$$

D_g is the gas phase mass diffusivity

The relation for energy conservation can be written in the following form

$$\frac{\partial (\rho h)}{\partial t} + \frac{1}{r^2} \frac{\partial}{\partial r} \left[r^2 \rho \left(v_r \cdot h - D \cdot C_p \frac{\partial T}{\partial r} \right) \right] = 0 \quad (4)$$

The energy or heat diffusion equation for the gas phase, equation (5) can be derived with the help of overall mass conservation equation (1) and equation (4), as:

$$\frac{\partial T}{\partial t} = \alpha_g \frac{\partial^2 T}{\partial r^2} + \frac{2\alpha_g}{r} \frac{\partial T}{\partial r} - v_r \left(\frac{\partial T}{\partial r} \right) \quad (5)$$

T is the temperature, α_g is gas phase thermal diffusivity. Neglecting radial velocity of fuel vapour v_r for the present model, equations (3) and (5) reduce to a set of linear, second order partial differential equations (eqns 6 and 7).

$$\frac{\partial Y}{\partial t} = D_g \frac{\partial^2 Y}{\partial r^2} + \frac{2D_g}{r} \frac{\partial Y}{\partial r} \quad (6)$$

$$\frac{\partial T}{\partial t} = \alpha_g \frac{\partial^2 T}{\partial r^2} + \frac{2\alpha_g}{r} \frac{\partial T}{\partial r} \quad (7)$$

These equations can be accurately solved with finite difference technique using appropriate boundary conditions and provide the solution in terms of species concentration profiles (fuel vapour and oxidiser) and temperature profile for the inflame and post flame zones respectively.

The boundary and initial conditions based on this combustion model are as follows

$$\text{at } r = r_f; T = T_f, Y_{o,f} = 0, Y_{F,f} = 0$$

$$\text{at } r = r_\infty; T = T_\infty, Y_{o,\infty} = 0.232,$$

$$\text{at } t = 0; r = r_{lo}, T = T_b, Y_{F,S} = 1.0$$

$$\text{where } r_i = r_{lo} (1 - t/t_d)^{1/2} \text{ for } (0 \leq t \leq t_d),$$

is the moving boundary condition coming out from the d^2 -law. Here, T_f and T_∞ are temperatures at the flame and ambient atmosphere respectively. $Y_{F,S}$ and $Y_{F,f}$ are fuel mass fractions respectively at the droplet surface and flame. $Y_{o,\infty}$ and $Y_{o,f}$ are oxidiser concentrations in the ambience and at the flame respectively, t is the instantaneous time, t_d is the combustion lifetime of the droplet, r_{lo} is the original or initial droplet radius and r_i is the instantaneous droplet radius at time “ t ”.

The location where the maximum temperature $T = T_f$ or the corresponding concentrations $Y_{F,f} = 0$ and $Y_{o,f} = 0$ occur, was taken as the flame radius r_f . Instantaneous time “ t ” was obtained from the computer results whereas the combustion lifetime “ t_d ” was determined from the relationship coming out from the d^2 -law. Other parameters like instantaneous flame to droplet diameter ratio (F/D), flame standoff distance $(F - D)/2$, dimensionless flame diameter (F / D_0) etc, were then calculated as a function of time. Products species concentrations (CO, NO, CO₂ and H₂O) were estimated using Olikara and Borman code [1] with gas phase code of the present study.

Solution technique

Equations (6) and (7) are a set of linear, second order, parabolic partial differential equations with variable coefficients. They become quite similar when thermal and mass diffusivities are made equal for unity Lewis number. They can be solved by any one of the following methods such as weighted residual methods, method of descritisation in one variable, variables separable method or by finite

difference technique. In weighted residual methods, the solution is approximate and continuous, but these methods are not convenient in present case since one of the boundary condition is time dependent. The method of discretisation in one variable is not suitable since it leads to solving a large system of ordinary differential equations at each step and therefore time consuming. Variables separable method provides exact and continuous solution but cannot handle complicated boundary conditions.

Keeping in view the limitations offered by other methods, “finite difference technique” is chosen (which can deal efficiently with moving boundary conditions, as is the case in present study) and successfully utilised in solving equations (6) and (7). The approach is simple, fairly accurate and numerically efficient [27]. Here the mesh size in radial direction is chosen as h and in time direction as k . Using finite difference approximations, equations (6) and (7) can be discretised employing three point central difference expressions for second and first space derivatives, and the time derivative is approximated by a forward difference approximation resulting in a two level, explicit scheme (eqn 8), which is implemented on a computer.

$$T_m^{n+1} = \alpha\lambda_1(1-p_m)T_{m-1}^n + (1-2\alpha\lambda_1)T_m^n + \alpha\lambda_1(1+p_m)T_{m+1}^n \quad (8)$$

Here, λ_1 (mesh ratio) = k/h^2 , $p_m = h/r_m$,

$$r_m = r_{io} + mh, \quad Nh = r_{\infty} - r_{io}, \quad m = 0, 1, 2, \dots, N.$$

The solution scheme is stable as long as the stability condition $\lambda_1 < 1/2$ is satisfied. Equations (6) and (7) can also be discretised in Crank-Nicholson fashion, which results in a six point, two level implicit scheme. From a knowledge of solution at the n^{th} time step, we can calculate the solution at the $(n+1)^{th}$ time step by solving a system of $(N-1)$ tridiagonal equations. Although the resulting scheme is more accurate, the cost of computation is fairly high.

Stability condition

The two level explicit scheme given by equation (8) with an order of accuracy $O(k+h^2)$ is stable for $\lambda_1 < 1/2$ and is reasonably accurate as long as stability criterion is obeyed as discussed below.

Applying Von-Neuman method [27], we write the error in the form $\epsilon_m^n = A \xi^n e^{i\theta mh}$ (9)

A is an arbitrary constant, ξ is the amplification factor and θ an arbitrary angle. Substituting ϵ_m^n in place of U_m^n in the equation

$$U_m^{n+1} = \alpha\lambda_1(1-p_m)U_{m-1}^n + (1-2\alpha\lambda_1)U_m^n + \alpha\lambda_1(1+p_m)U_{m+1}^n$$

we obtain

$$\epsilon_m^{n+1} = \alpha\lambda_1(1-p_m)\epsilon_{m-1}^n + (1-2\alpha\lambda_1)\epsilon_m^n + \alpha\lambda_1(1+p_m)\epsilon_{m+1}^n \quad (10)$$

The solution of the above equation determines the growth of error in the computed values of U_m^n . Substituting from (9) into (10), we obtain after simplification:

$$\xi = 2\lambda_1 \cos \theta h + \lambda_1 p_i \sin \theta h + (1 - 2\lambda_1).$$

For stability, $|\xi|$ is less than 1, so that the error remains bounded and does not tends to infinity. This condition is only satisfied if $\lambda_1 < 1/2$.

2.2 Estimation of flame temperature

In the present work, thermodynamic and transport properties were evaluated on the basis of flame temperature and ambient temperature for the outer or the post flame zone and boiling point temperature and flame temperature for the inner or inflame zone. Accuracy of the evaluated properties depend upon the correct estimation of flame temperature and play a vital role in predicting combustion parameters and their comparison with the experimental results. A computer code was developed in the present work for determining the adiabatic flame temperature using first law of thermodynamics with no dissociation effects. A more accurate method like Gülder [28] (described below) which incorporates dissociation, multicomponent fuels and high temperature and pressure effects was also used for getting flame temperature. An expression of the following form has been adopted to predict the flame temperature, which is applicable for the given ranges:

$$[0.3 \leq \phi \leq 1.6; 0.1 \text{MPa} \leq P \leq 7.5 \text{MPa}; 275 \text{K} \leq Tu \leq 950 \text{K}; 0.8 \leq H/C \leq 2.5]$$

$$T_{adiabatic} = A\sigma^\alpha \cdot \exp\left[\beta(\sigma + \lambda)^2\right] \cdot \pi^x \theta^y \psi^z \quad (11)$$

where,

$$x = a_1 + b_1\sigma + c_1\sigma^2$$

$$y = a_2 + b_2\sigma + c_2\sigma^2$$

$$z = a_3 + b_3\sigma + c_3\sigma^2$$

π is dimensionless pressure = P/P_o ($P_o = 0.1013 \text{MPa}$)

θ is dimensionless initial mixture temperature
 $= T_u / T_a$

$$T_a = 300 \text{ K}$$

ψ is H / C atomic ratio

$\sigma = \phi$ for $\phi \leq 1$ (ϕ is the fuel-air equivalence ratio defined as

$$(F / A)_{\text{actual}} / (F / A)_{\text{stoichiometric}})$$
 and

$$\sigma = \phi - 0.7, \text{ for } \phi > 1$$

$$\text{Now, } T_u = \frac{C_{pf} T_l + (A / F) C_{pa} T_a - L}{C_{pf} + (A / F) C_{pa}} \quad (12)$$

C_{pf} is the specific heat of fuel vapour

C_{pa} is the specific heat of air obtained from standard air tables

T_l is the liquid fuel temperature

$$C_{pf} = (0.363 + 0.000467 \cdot T_b)(5 - 0.001 \rho_{fo}) \quad (\text{kJ/kgK})$$

ρ_{fo} is density of fuel at 288.6 K

T_b is boiling point Temperature (K)

$$\psi = 0.9479 [T_{mb} / 100]^{0.2527} \cdot [\rho_f]^{-2.4063}$$

T_{mb} is the fuel mid boiling point (K)

ρ_f is the relative liquid density of fuel at 20 °C

$$L = (360 - 0.39 T_l) / \rho_f \quad (\text{kJ / kg}) \quad (13)$$

(latent heat of vaporization L can also be evaluated from Reid et al. [29])

Once ϕ and θ are known, Table A.1 [28] given in Appendix A can be consulted for choosing constants $A, \alpha, \beta, \lambda, a_1, b_1, c_1, a_2, b_2, c_2, a_3, b_3, c_3$ to be used in equation (11).

After determining the flame temperature, the reference or average temperatures for the inflame and post flame zones respectively can be calculated using average values given as:

$$T_{ref1} = (T_b + T_f) / 2 \text{ and } T_{ref2} = (T_f + T_\infty) / 2 \quad (14)$$

or by using 1/3 rule [30], given as:

$$T_{ref1} = (1/3) T_b + (2/3) T_f \text{ and}$$

$$T_{ref2} = (1/3) T_f + (2/3) T_\infty \quad (15)$$

For the present gas phase model, thermodynamic and transport properties like specific heats, diffusion coefficients, thermal conductivities, latent heats, densities, were evaluated as a function of reference temperature and pressure from different correlations along with proper mixing rules [29]. Combustion parameters like heat transfer number B_T , burning

constant k_b , combustion lifetime of the droplet t_d and mass burning rate m_f were then calculated on the basis of these properties. Effects of forced convection and droplet heating were also incorporated.

2.3 Temperature and species concentration profiles for a spherically symmetric combusting droplet at the start of droplet burning ($t / t_d = 0$)

The solution of energy equation (7) was obtained in the form of temperature profiles covering the inflame and post flame regions. Droplet surface temperature was assumed equal to the boiling point temperature T_b of the fuel. Fig. 2 indicates that the temperature profile starts from the boiling point temperature (371.6 K), reaches a maxima at the flame zone where T_f is equal to 2396.17 K and then gradually decreases to the ambient temperature value of 298 K. The radius at which the maximum flame temperature T_f occurs is the corresponding flame radius r_f . For simplicity, the flame temperature was calculated using first law of thermodynamics with no dissociation effects using a computer programme developed in the present work. The temperature profile was obtained through computed results for one particular time of droplet burning, when $t / t_d = 0$, that is, the time when the combustion has just started ($t = 0$).

Species concentration profiles (fuel vapour concentration profile for the inflame zone and oxidiser concentration profile for the post flame zone) were obtained by solving the species diffusion equation (equation 6) numerically. In Fig. 2, the computed results indicate that in the inflame zone, the fuel vapour concentration is maximum at the droplet surface, i.e. $Y_{F,S} \approx 1$, and gradually decreases to zero at the flame ($Y_{F,f} = 0$). The oxidiser (oxygen) diffuses from the ambient atmosphere in the post flame zone where its concentration is 23.2 % ($Y_{O,\infty} = 0.232$) and gradually reduces to zero at the flame ($Y_{O,f} = 0$). Both fuel vapour and oxidiser are consumed at the flame. Temperature and concentration profiles obtained at different times of droplet burning are shown in Fig. 3.

2.4 Temperature and species concentration profiles at different times of droplet burning.

Fig. 3 shows complete history of droplet burning from beginning of the combustion process ($t/t_d = 0.0$) till the end of droplet burning ($t/t_d = 0.9$). It is

observed that initially the flame is very near to the droplet surface, then it moves away from the droplet and finally comes very close to the droplet surface again at the end of droplet lifetime. This behaviour is consistent with the experimental results [4,5].

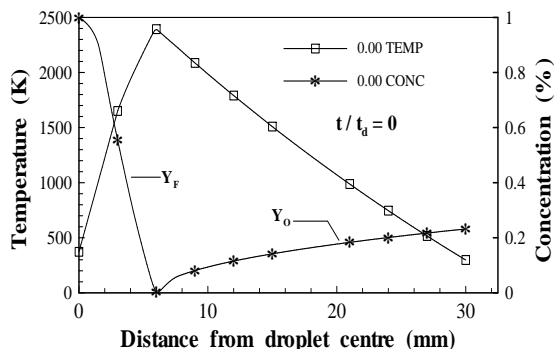


Fig. 2. Temperature and concentration profiles for n-heptane in radial direction ($D_0 = 2000$ microns, $T_\infty = 298$ K, $P_\infty = 1$ atm, $Y_{o,\infty} = 0.232$).

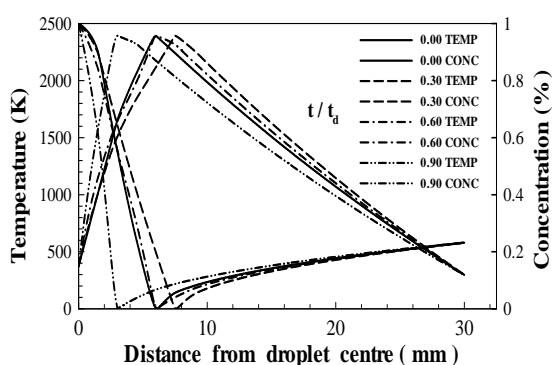


Fig. 3. Temperature and concentration profiles at different droplet burning times.

2.5 Flame diameter F and square of droplet diameter D^2 behaviour with instantaneous time

Variation of F and D^2 with t for a 930 micron ethanol droplet is shown in Fig 4. The present result is compared with that of Hara and Kumagai [4] who conducted experimental investigations of free droplet combustion under microgravity with n-heptane and ethyl alcohol. The comparison shows that for the same fuel, droplet size and ambient conditions, there is a general agreement between the results of the two studies, that is, the flame diameter F first increases and then decreases and the square of droplet diameter decreases linearly with time.

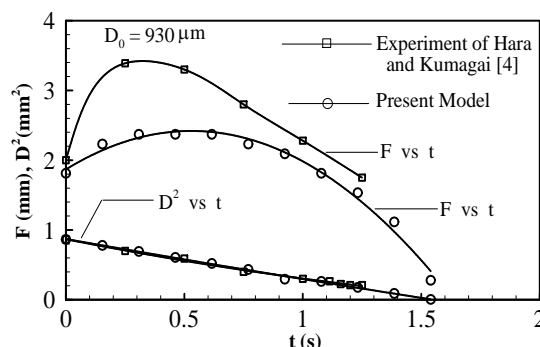


Fig. 4. Flame diameter and square of droplet diameter versus time for ethanol droplet burning in standard atmosphere.

2.6 F/D ratio variation with time

In Fig. 5, F/D ratio is plotted against instantaneous time t for a 1336 micron n-heptane droplet burning in standard atmosphere. It is observed that the results of the present model are close to those of Okajima and Kumagai [5] who investigated the combustion of free n-heptane droplets in microgravity conditions in a freely falling chamber. The small difference may be due to the calculated values of thermodynamic properties which are subsequently used in the gas phase code of the present model to get flame diameter F , whereas the instantaneous droplet diameter $D = 2r_i$ is obtained from the relation $r_i = r_{i0} (1 - t/t_d)^{1/2}$. Both results indicate that F/D ratio continuously increases from the beginning of combustion till the end of droplet lifetime, thereby suggesting that droplet combustion is a transient phenomenon unlike the quasi-steady model where F/D ratio comes out as a large constant value of the order of 35.53 using equation provided by the quasi-steady burning:

$$F/D = \ln[1 + B_T] / \ln[(\nu + 1) / \nu] \quad (16)$$

For equation (16), ν is the $(A/F)_{stoich}$ on mass basis equal to 15.1. B_T for steady state burning was calculated as 8.765 using equation (24) with no droplet heating effect:

$$B_T = \Delta h_c / \nu + \bar{C}_{pg} (T_\infty - T_b) / L.$$

In the quasi-steady model, the droplet and flame diameters are fixed and neither D nor F are changing with time. In other words, the quasi-steady model is a simulation of the porous sphere experiment, where the fuel is fed at a constant rate to a ceramic sphere (representing a droplet) and the flame is fixed relative to the droplet centre. Therefore in droplet combustion studies, the flame movement cannot be predicted with the assumption of quasi-steady gas phase.

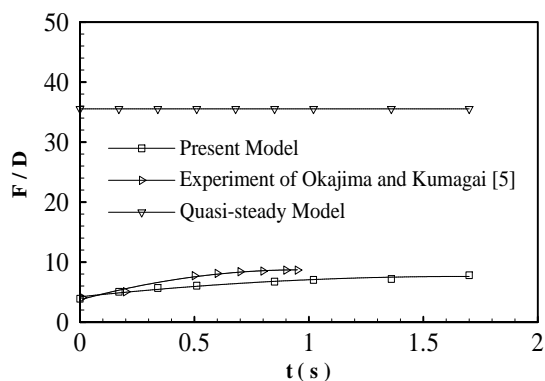


Fig. 5. Flame to droplet diameter ratio versus time for a 1336 micron n-heptane droplet burning in standard atmosphere.

2.7 Flame diameter F against droplet diameter D

Considering Fig. 6, for the same fuel (n-heptane) and burning conditions, with $D_0 = 2000$ microns, the result of the present model shows that flame diameter F increases from an initial value of 1.2cm to a maximum of 1.5cm, then flame diameter decreases gradually to a value of 0.48cm. The corresponding value of droplet diameter D is maximum at the onset of combustion being equal to the original droplet diameter D_0 (0.2cm), after that it decreases to a minimum value of about 0.04cm. This variation is in agreement with the experimental results where flame diameter first increases and then decreases while droplet diameter decreases continuously from beginning to the end of droplet burning period.

2.8 Extension of spherically symmetric gas phase droplet combustion model to convective environment

Typical conditions of hydrocarbon fuel droplets in combustion chambers may have high temperatures of 1000 K or more, relative velocity between the droplet surface and ambient gas ≈ 10 m/s and Reynolds number based on relative velocity and gas properties can be of the order of 100.

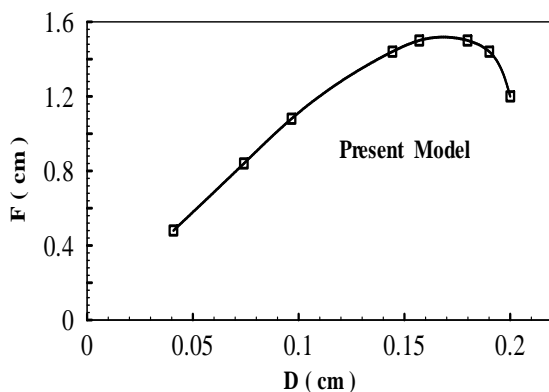


Fig. 6. Variation of flame diameter with droplet diameter.

Droplet combustion in convective environment can be studied in a simpler way by considering a spherical droplet vaporising with a radial flow field in the gas phase and then correcting the result with an empirical correlation for forced convection which is a function of dimensionless parameters such as Reynolds number, Prandtl number [6].

For analysing convective droplet combustion, the following procedure was adopted. The adiabatic flame temperature T_f was first obtained by considering stoichiometric reaction between air and fuel (n-octane) using first law of thermodynamics with no effects of dissociation. The gas phase mixture properties were then calculated at the average temperature of T_f and T_∞ and finally corrected by applying proper mixing rules.

T_f for n-octane was calculated as 2395K. μ for n-octane fuel vapour as a function of temperature was determined by Lucas method, μ_{air} as a function of temperature was taken from [31]. Then absolute viscosity of the mixture $\mu_{g(air+fuel\ vapour)}$ or $\bar{\mu}_\infty$ as a function of temperature was determined from mixing rules using Wilke method [29], as $\bar{\mu}_\infty = 5.1483 \times 10^{-5} \text{ N s / m}^2$. Other mixture properties as a function of temperature were calculated likewise (using appropriate correlations). Gas phase Reynolds number based on droplet diameter is given as:

$$Re_g = D_0 U_\infty \bar{\rho}_\infty / \bar{\mu}_\infty \quad (17)$$

D_0 is the original droplet diameter, U_∞ is the relative velocity between the droplet surface and the ambient gas taken as 10 m/s, $\bar{\rho}_\infty$ is the density of the mixture = 0.399 kg/m³. For a chosen droplet diameter of 1300 μm (1.3mm), we get $Re_g \approx 100$. Then,

$$Pr_g = \bar{C}_{pg} \times \bar{\mu}_\infty / \bar{\lambda}_g = 2766 \times 5.1483 \times 10^{-5} / 0.0768 = 1.854. \quad (18)$$

Here mixture specific heat \bar{C}_{pg} is in J/kgK and mixture thermal conductivity $\bar{\lambda}_g$ is in W/mK.

Following cases were considered :

(a) Droplet heating with no convection

Then using equation for transfer number:

$$B_T = \frac{\Delta h_c / \nu + \bar{C}_{pg} (T_\infty - T_b)}{L + C_{pl} (T_b - T_\infty)} \quad (19)$$

Δh_c is the heat of combustion of fuel = 44425 kJ/kg

ν is the $(A/F)_{stoch}$ on mass basis = 15.05

C_{pl} as a function of temperature was calculated as
 2.15 kJ/kgK

L is the latent heat of vaporisation of fuel
 = 301.92 kJ/kg

T_b is the boiling point of fuel = 399 K,

$T_\infty = 298K$

hence, heat transfer number $B_T = 5.148$

using equation (19) for droplet heating, with
 $B_T = 5.148$,

$$t_d = \frac{\rho_l D_0^2}{8\lambda_g / \bar{C}_{pg} \ln(1+B_T)} \quad (20)$$

(here, ρ_l is density of liquid = 703 kg/m³),

D_0 is original droplet diameter. Hence, we have

$$t_d = 2.945 \text{ s}.$$

Equation (21) gives the variation of instantaneous droplet radius r_l with instantaneous time "t" ;

$$\int_{r_o}^{r_l} r_l dr_l = -\frac{\lambda_g}{\bar{C}_{pg} \rho_l} \ln(1+B_T) \int_{t=0}^{t_d} dt \quad (21)$$

Finally, the mass burning rate as a function of time can be calculated using equation (22),

$$m_f = \pi r_l \rho_l k_b / 2 \quad (22)$$

(b) Droplet heating with convection

Here, t_d is modified using equation (20), as

$$t_d = \frac{\rho_l D_0^2}{8\lambda_g / \bar{C}_{pg} \ln(1+B_T) (1+0.3Re_g^{0.5} Pr_g^{0.33})} = 0.629 \text{ s} \quad (23)$$

(with

$$B_T = 5.148, Re_g = 100 \text{ and } Pr_g = 1.854)$$

The variation of droplet radius with time can be determined from equation (21) and mass burning rate from equation (22).

(c) No droplet heating and no convection (steady state combustion)

B_T at steady state condition is given as:

$$B_{T_{ss}} = \Delta h_c / \nu + \bar{C}_{pg} (T_\infty - T_b) / L \quad (24)$$

Then, $B_{T_{ss}} = 8.851$ and using equation (20),

$$t_{d_{ss}} = 2.33 \text{ s}.$$

Variation of droplet radius with time can be determined directly from $d^2 - law$

$$r_l = r_{lo} (1 - t / t_d)^{1/2} \quad (25)$$

and as before, mass burning rate from equation (22).

The results are shown in Figs. 7-12. Figs. 7 to 9 show the variation of square of instantaneous droplet diameter D^2 with instantaneous time t , for a n-octane droplet of 1.3 mm diameter. For the case when there is steady state burning, (Fig. 7) that is no droplet heating and no effects of convection, it is observed that there is a linear variation of D^2 with t and the droplet is consumed in approximately 2.4s. Whereas, in Fig. 8, due to droplet heating, droplet lifetime is increased to about 3 seconds for the same fuel and burning conditions, however D^2 versus t variation is still linear ($d^2 - law$ is followed). Fig. 9 shows that when both droplet heating and convection are considered, droplet is consumed in a very short time of about 0.63s. If there had been no droplet heating in presence of convection, then the lifetime would have been even lesser.

Figs. 10-12 depict for the same conditions of fuel, droplet size and ambient conditions the variation of droplet mass burning rate m_f with instantaneous time t . From Fig. 10, where there is no droplet heating and no convection, mass burning rate is about 0.5 mg/s initially. In Fig. 11, when droplet heating is considered, the initial mass burning rate is less than the previous case. This is because as the droplet heats up to its boiling point, the quantity of fuel vapour evaporating from the droplet surface is small and hence mass burning rate is reduced.

Fig. 12 shows the variation of m_f with t when convection is considered with droplet heating. It is observed that there is an abrupt change in the values of mass burning rate and droplet lifetime. Due to the presence of convection the initial mass burning rate jumps to a value of about 1.92 mg/s and droplet is consumed in a very short time. Further, if droplet heating had been ignored in this case, then the initial mass burning rate would have increased further.

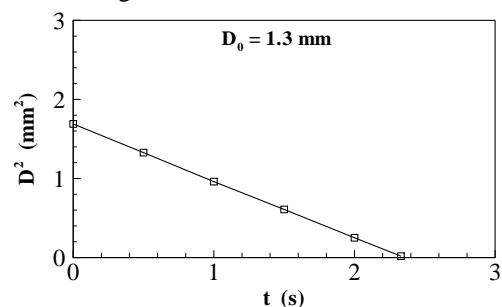


Fig. 7. Square of droplet diameter variation with time for n-octane neglecting droplet heating and convection ($P_\infty = 1 \text{ atm}$, $T_\infty = 298 \text{ K}$, $Y_{o,\infty} = 0.232$).

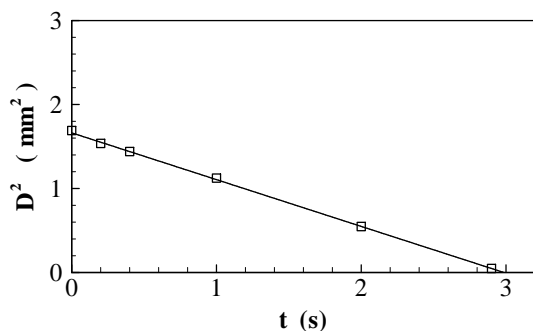


Fig. 8. Droplet heating with no convection

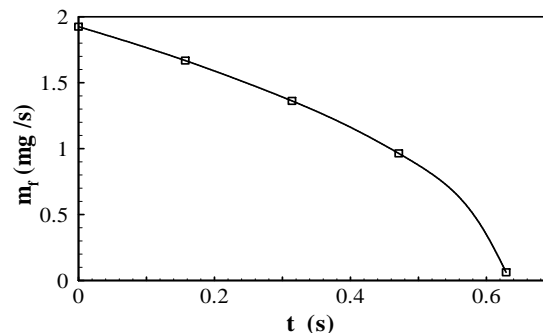


Fig. 12. Droplet heating with convection.

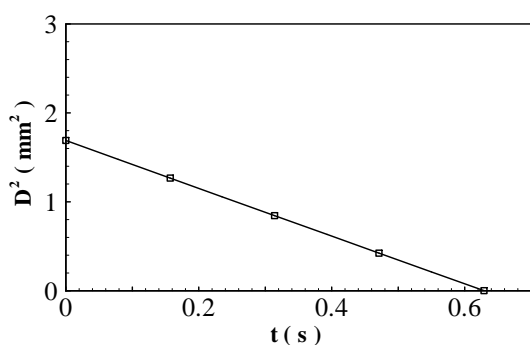


Fig. 9. Droplet heating with convection.

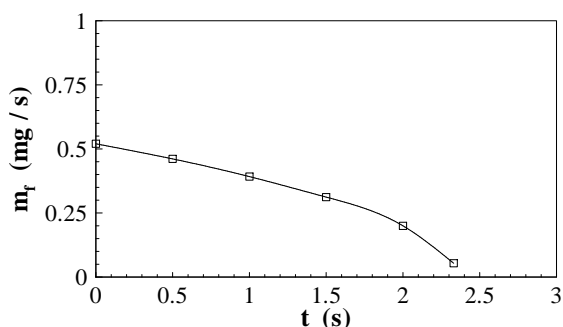


Fig. 10. Mass burning rate versus time for n-octane neglecting droplet heating and convection.

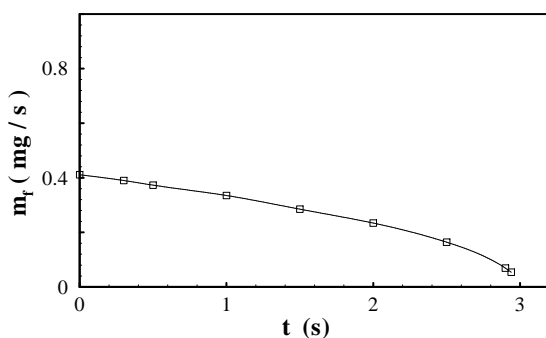


Fig. 11. Droplet heating without convection.

III. Determination of emission data for a spherically symmetric burning droplet

Most experiments related to droplet burning have been concerned primarily with combustion aspects such as measurement of droplet and flame temperatures, flame movement, droplet lifetimes, burning rates etc. As a result less experimental data related to emission characteristics is available in literature. Such information is needed to examine the formation and destruction of pollutants such as soot, unburned hydrocarbons, NO_x, CO and CO₂ and subsequently to establish design criteria for efficient and stable combustors.

For the determination of species concentration profiles around the burning spherical droplet, the following procedure was adopted.

Adiabatic flame temperature determined earlier, using first law of thermodynamics together with other input data was used to solve numerically, the gas phase energy equation (7) with the help of a computer programme. The solution obtained was in the form of temperature profile at each time step starting from the droplet surface, reaching the maxima at the flame and then reducing to the ambient temperature value. The radius at which the maximum temperature occurred was taken as the flame radius.

Temperature values in the vicinity of the flame were then chosen from the computed results, which were designated as number of steps (*NOS*). The solution of species diffusion equation (6) in the gas phase, gave the species profile (fuel and oxidiser). It was observed that the fuel vapour concentration was maximum at the droplet surface and decreased gradually to the minimum value at the flame front, whereas, oxygen diffusing from the ambient atmosphere became minimum at the flame. Now for the same time step, which was used in the solution of energy equation, values or *NOS* of fuel mass fraction Y_F corresponding to the temperature values

were taken from the computed results of the species diffusion equation.

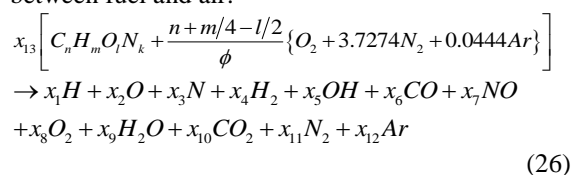
Then for a particular fuel, *FARS* (fuel to air ratio stoichiometric) on mass basis was calculated for the stoichiometric reaction of fuel and air at atmospheric conditions of temperature $T_\infty = 298K$, pressure $P_\infty = 1 \text{ atmosphere}$ and ambient oxidiser concentration $Y_{O,\infty} = 0.232$.

Fuel to air ratio actual (*FARA*) on mass basis was then calculated for each step where, $FARA = Y_F / 1 - Y_F$, and finally equivalence ratio, $\phi = FARA / FARS$. The values of flame temperature, equivalence ratio and ambient pressure were then used as input data for the Olikara and Borman Code [1], (modified for single droplet burning case) to obtain concentrations of important combustion products species.

Moreover, since most of the practical combustion systems operate with air as an oxidiser therefore formation of NO is a significant parameter which was another reason for our preference for the Olikara and Borman programme [1].

3.1 Chemical Equilibrium Composition

The Olikara and Borman model [1] considered combustion reaction between fuel $C_n H_m O_l N_k$ and air at variable fuel-air equivalence ratio ϕ , temperature T and pressure P . Following equation was considered for representing combustion reaction between fuel and air:



Where x_1 through x_{12} are mole fractions of the product species and n, m, l and k are the atoms of carbon, hydrogen, oxygen and nitrogen respectively in the fuel. The number n and m should be non-zero while l and k may or may not be zero.

The number x_{13} , represents the moles of fuel that will give one mole of products. In addition to carbon and hydrogen, the fuel may or may not contain oxygen and nitrogen atoms. In the present study, fuels considered were free from nitrogen atoms. The product species considered [1] were $H, O, N, H_2, OH, CO, NO, O_2, H_2O, CO_2, N_2$ and

Ar in gas phase. Whereas in the present work, only CO, NO, CO_2 and H_2O were considered for the sake of simplicity.

The equilibrium constants used in the programme [1] were fitted as a function of temperature in the range (600K – 4000K). It was shown that equivalence ratio,

$$\phi = \frac{AN + 0.25AM - 0.5AL}{0.5AN - 0.5AL} \quad (27)$$

(where AN, AM, AL are the number of C, H and O atoms in fuel molecules). The products of combustion were assumed to be ideal gases (assumption not valid at extremely high pressures). The gas phase code developed in the present work was used with the Olikara and Borman code [1] for calculating the equilibrium composition of combustion products representing species concentration profiles around a burning droplet. Important steps of this programme and detailed kinetic mechanism are given in [1].

3.2 Emission characteristics

The behaviour of species concentrations as a function of dimensionless flame radius r/r_f across the flame zone with finite thickness is shown in Fig. 13. The general mechanism of formation of products involves the conversion of the reactants to CO and H_2 on the fuel rich side. The CO and H_2 further diffuse towards the thin reaction zone, which is the flame sheet and react with increasing amount of O_2 and get oxidised to form CO_2 and H_2O . The instantaneous temperature at the given point may affect the mechanism and the rate of these reactions. It is observed that NO concentration is maximum at the flame zone and is found to be very temperature sensitive. Results of the present study show higher than expected concentrations. However, the present work aims at providing a qualitative trend rather than quantitative using a simplified approach.

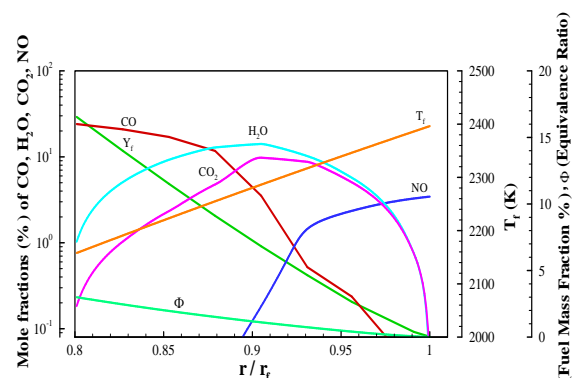


Fig. 13. Emission characteristics of n-heptane droplet ($D_0=100$ microns) burning at 1 atm and 298 K.

IV. Liquid phase analysis

For the development of liquid phase model “conduction limit” approach was followed where conduction is the only mode of heat transport from the energy arriving at the droplet surface to its

interior. Combustion of a n-octane liquid droplet in ambient conditions of one atmosphere pressure and 298 K was considered. Here, the droplet temperature is varying both spatially and temporally. The system is spherically symmetric with no internal liquid motion. Gas phase is assumed quasi-steady. Clausius-Clapeyron relation describes the phase equilibrium at the liquid-vapour interface. The spherically symmetric, liquid phase heat diffusion equation or energy equation is given as:

$$\frac{\partial T_l}{\partial t} = \frac{\alpha_l}{r^2} \frac{\partial}{\partial r} \left(r^2 \frac{\partial T_l}{\partial r} \right) = \alpha_l \left[\frac{\partial^2 T_l}{\partial r^2} + \frac{2}{r} \frac{\partial T_l}{\partial r} \right] \quad (28)$$

T_l and α_l are liquid phase temperature and thermal diffusivity respectively.

Initial and boundary conditions being

$$T(r, 0) = T_0(r) \quad (29)$$

$T_0(r)$ is the initial temperature distribution

$$\left(\frac{\partial T}{\partial r} \right)_{r=0} = 0 \quad (30)$$

$$mH = mL + \left(4\pi^2 \lambda_l \frac{\partial T}{\partial r} \right)_{r_s} \quad (31)$$

Where r_s is the radius at the droplet surface, λ_l is the liquid thermal conductivity.

The above equation represents the energy conservation at the interface, L and H are specific and effective latent heat of vaporisation respectively. Spherically symmetric, multicomponent liquid phase mass diffusion equation with no internal circulation is:

$$\frac{\partial Y_{l,m}}{\partial t} = D_l \left(\frac{\partial^2 Y_{l,m}}{\partial r^2} + \frac{2}{r} \frac{\partial Y_{l,m}}{\partial r} \right) \quad (32)$$

$Y_{l,m}$ is the concentration or mass fraction of the m th species in the liquid, and D_l is liquid mass diffusivity which in this case is much smaller than liquid phase thermal diffusivity α_l , hence liquid phase Lewis number, $Le_l \gg 1$.

The boundary condition at the liquid side of the droplet surface is:

$$\left. \frac{\partial Y_{l,m}}{\partial r} \right|_s = \frac{\rho_g D_g}{\rho_l D_l r_i} \ln [1 + B] [Y_{l,ms} - \varepsilon_m] \quad (33)$$

m denotes particular species, r_i is the instantaneous droplet radius at time "t", ε_m is species fractional mass vaporisation rate,

B is the transfer number, D_l and D_g are liquid and gas phase mass diffusivities respectively, ρ_l and ρ_g are respectively the liquid and gas phase densities;

At the centre of the droplet, symmetry yields

$$\left. \frac{\partial Y_{l,m}}{\partial r} \right|_{r=0} = 0 \quad (34)$$

A uniform initial liquid phase composition for the droplet was chosen, given as:

$$Y_{l,m}(0, r) = Y_{l,mo} \quad (35)$$

Equations (28) and (32) are linear, second order partial differential equations. A convenient method of solving problems with moving boundary is to change the moving boundary to a fixed boundary using coordinate transformation. Hence, equations (28) and (32) along with the boundary conditions (equations 28-35) are transformed and solved numerically using finite difference technique.

The Clausius-Clapeyron relation can be written as [32]:

$$Y_{F,S} = \{ (1 + W_g / W_F (P_\infty \exp([C_{pg} / R][1/\hat{T}_s - 1/\hat{T}_b]) - 1))^{-1} \} \quad (36)$$

W_g is the average molecular weight of all gas phase species except fuel, at the surface, W_F is the molecular weight of the fuel. R is the specific gas constant of the fuel, P_∞ is equal to one atmosphere, \hat{T}_s and \hat{T}_b dimensionless droplet surface and boiling point temperatures respectively.

Equation (32) with boundary conditions must be applied concurrently with phase equilibrium conditions and heat diffusion equation (28) to obtain the complete solution. For a single component fuel, phase equilibrium can be expressed by the Clausius-Clapeyron equation and ε_m (species fractional mass vaporization rate) is unity. For a multicomponent fuel, Raoult's law provides for the phase equilibrium and $\varepsilon_m \neq 1$.

4.1 Plot of centre and surface temperatures within the liquid droplet

The solution of energy equation provides a plot of droplet surface and centre temperatures as a function of radial distance at different times of droplet burning or droplet vaporisation, as the case may be. The variation of droplet surface temperature with time then becomes an important input parameter for the solution of liquid phase mass diffusion equation.

Fig. 14 shows temperature profiles within a spherically symmetric n-octane liquid droplet burning in standard atmosphere. It is observed that as dimensionless time is increased from an initial value to about 0.4, droplet surface and center temperatures become equal to a value corresponding to approximately 383 K. The droplet heating time is about 23%. In other words, the heat energy arriving from the flame is now fully utilized for surface evaporation and none of the heat is conducted inside for the purpose of droplet heating, suggesting the onset of steady state combustion. Fig. 15 depicts the results of Law and Sirignano [32] for the same burning conditions. Other important droplet parameters required are the gas side mole and mass fractions of each species, transfer number, species fractional mass vaporisation rate ϵ_m and thermodynamic properties of the multicomponent fuel.

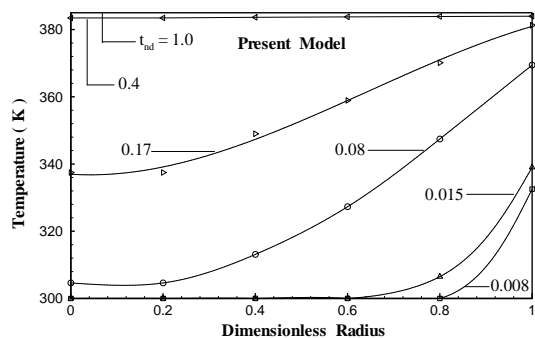


Fig. 14. Temporal and Spacial Variations of Liquid temperatures

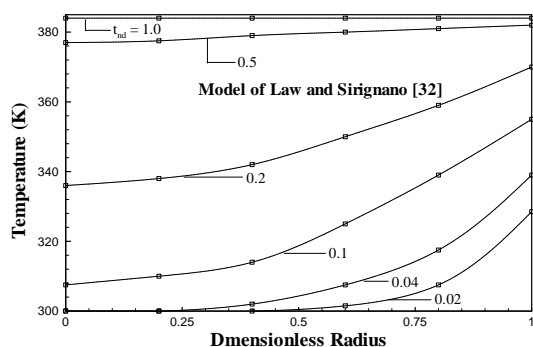


Fig. 15. Modelling results of Law and Sirignano.

V. Development of droplet vaporisation model at high pressure

Combustion chambers of diesel engines, gas turbines and liquid rockets operate at supercritical conditions. To determine evaporation rates of liquid fuel sprays (made up of discrete droplets) at high pressures, a prior thermodynamic analysis is a must. Important assumptions employed in the present high pressure model are:

Droplet shape remains spherical, viscous dissipation effects are neglected, ambient gas gets

dissolved in the droplet surface layer only, gas phase behaves in a quasi-steady manner, radiation heat transport is neglected and Soret and Dufour effects are not considered.

At high pressures, vapour-liquid equilibria for each component can be expressed as:

$$\begin{aligned} f_1^{(v)} &= f_1^{(l)} \\ T^{(v)} &= T^{(l)} \end{aligned} \quad (37)$$

where, the superscripts (v) and (l) stand for vapour and liquid respectively.

f_i is the fugacity for component or species “i” and can be integrated through the following relation

$$R_u T \ln \frac{f_i}{x_i P} = \int_V^\infty \left[\left(\frac{\partial P}{\partial n_i} \right)_{T,V,n_j} - \frac{R_u T}{V} \right] dV - R_u T \ln Z \quad (38)$$

The above equation suggests that f_i can be determined by the properties of the constituent components, the concentrations in both phases and the temperature and pressure of the system. To compute the integral of the above equation, a real gas equation of state such as Redlich-Kwong equation of state was chosen which is given as:

$$P = \frac{R_u T}{v-b} - \frac{a}{v(v+b)T^{0.5}} \quad (39)$$

Equation (38) is then integrated. After

simplification we get an equation of the form:

$$\ln f_i = \ln x_i + \ln P + \frac{b_i}{b} (Z-1) - \ln(Z-B) - \frac{A}{B} \left[\frac{2 \sum_{j=1}^N x_j a_{ij}}{a} - \frac{b_i}{b} \right] \ln \left(1 + \frac{B}{Z} \right) \quad (40)$$

This equation is valid for both vapour and liquid phases. The dimensionless parameters A and B are defined as:

$$A = \frac{aP}{R_u^2 T^2} \quad \text{and} \quad B = \frac{bP}{R_u T} \quad (41)$$

Redlich-Kwong equation can be written in the form of compressibility factor as:

$$Z^3 - Z^2 + (A - B - B^2)Z - AB = 0 \quad (42)$$

The mixture compressibility factor “Z” can be determined using Cardan’s method, where highest value of Z corresponds to vapour phase and the smallest value to liquid phase. The parameters a and b in the cubic equation can be expressed in terms of composition and pure component parameters as:

$$a = \sum_{i=1}^2 \sum_{j=1}^2 x_i x_j a_{ij}, \quad b = \sum_{i=1}^2 x_i b_i \quad (43)$$

The constants a_{ij} and b_i are essentially dependent on the critical properties of each species. In addition, proper mixing rules have to be employed to determine various mixing parameters for different mixtures.

Equation (40) can be rewritten for components 1 and 2 respectively and can be applied to both vapour and liquid phases. For a two component, two phase system in equilibrium at a given temperature and pressure, there are four mole fractions $x_1^{(v)}$, $x_2^{(v)}$, $x_1^{(l)}$ and $x_2^{(l)}$ as unknowns for the phase equilibrium system. Now since equation (40) can be written for liquid and vapour phases for component 1 and at equilibrium, $f_1^{(l)} = f_1^{(v)}$, we get a relationship between $x_1^{(v)}$ and $x_1^{(l)}$. In the same manner, we can obtain a relation between $x_2^{(v)}$ and $x_2^{(l)}$. Further, in a mixture, $x_1^{(l)} + x_2^{(l)} = 1$ and $x_1^{(v)} + x_2^{(v)} = 1$, hence the four unknowns can be determined by solving two non linear equations iteratively. A suitable method which can be utilised is that of Newton-Raphson.

The solution of these equations was obtained in the form of a thermodynamic diagram representing vapour-liquid phase equilibrium compositions for a particular system at various pressures given below.

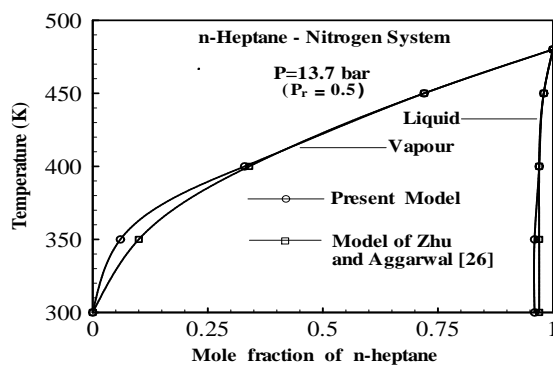


Fig. 16. Vapour-liquid phase equilibrium compositions predicted by Redlich-Kwong equation of state for n-heptane-nitrogen system.

For complete solution, variation of D^2 with t and droplet lifetime can also be determined. Proper estimation of thermophysical and transport properties are essential especially for multicomponent, high pressure, high temperature studies since simulation results depend heavily upon the correct evaluation of properties. For the present work, it was observed that in general the error was within 10% of the experimental values.

VI. Conclusions

From the literature review concerning single droplet combustion, it is observed that available droplet models are either too complicated or oversimplified for their successful incorporation in spray codes. The present work has tried to overcome this deficiency by evolving droplet sub models which are simple but preserve the essential physics and can be readily employed in CFD codes.

A comprehensive unsteady, spherically symmetric, single component gas phase droplet combustion model has been developed first by solving time dependent conservation equations of energy and species numerically with one initial and three boundary conditions. Results indicate that flame first moves away from the droplet surface then towards it, and flame stand off ratio (flame to droplet diameter ratio) increases throughout the burning period.

These results are in conformity with the experimental observations. Other authors have developed droplet combustion models that utilise three or four time dependent conservation equations together with phase equilibrium relations and three to four initial and boundary conditions. These equations are then non dimensionalised and solved either analytically or numerically and come up with the same results as in the present work. Present results being closer to the experimental observations.

The present gas phase model was then extended to include effects of forced convection and droplet heating and subsequently emission data.

This model can be further used to quantify the effects of ambient temperature, pressure composition, droplet size and fuels on the burning characteristics of single droplets.

The present work also provides the methodology for developing realistic multicomponent and high pressure droplet vaporisation/combustion models with a simplified approach.

The different sub-models are evolved with the main objective of their implementation in spray codes for enhancing the performance of practical combustion devices [33]. They are quite accurate and are represented by computer programmes that require less CPU time which is important in spray combustion involving large number of droplets.

References

- [1] C. Olikara, G. L. Borman, SAE Trans. (1975) SAE Paper 750468.
- [2] W. A. Sirignano, *Fluid Dynamics and Transport of Droplets and Sprays*, Cambridge University Press, 1999.
- [3] J. S. Chin, A.H. Lefebvre, AIAA Journal. 21 (10) (1983) 1437-1443.
- [4] H. Hara, S. Kumagai, Proc. Combust. Inst. 23 (1990) 1605-1610.

- [5] S. Okajima, S. Kumagai, Proc. Combust. Inst. 15 (1974) 401-407.
- [6] G. M. Faeth, Progress in Energy and Combust. Sci. 3 (1977) 191-224.
- [7] S. Kumagai, H. Isoda., Proc. Combust. Inst. 6 (1957) 726-731.
- [8] H. Isoda, S. Kumagai, Proc. Combust. Inst, 7 (1959) 523-531.
- [9] C. H. Waldman, Proc. Combust. Inst. 15 (1974) 429-442.
- [10] S. Ulzama, E. Specht, Proc. Combust. Inst. 31 (2007) 2301-2308.
- [11] I. K. Puri, P. A. Libby, Combust. Sci. Technol. 76 (1991) 67-80.
- [12] M. K. King, Proc. Combust. Inst. 26 (1996) 1227-1234.
- [13] J. R Yang, S. C. Wong, Int. J. Heat Mass Transfer. 45 (2002) 4589-4598.
- [14] C. K. Law, Combust. Flame. 26 (1976) 219-233.
- [15] R. B. Landis, A. F. Mills, Fifth Intl. Heat Transfer Conf. (1974), Paper B7.9, Tokyo, Japan.
- [16] C. K. Law, AIChE Journal. 24 (1978) 626-632.
- [17] A.Y. Tong, W. A. Sirignano, Combust. Flame. 66 (1986) 221-235.
- [18] P. Lara-Urbaneja, W. A. Sirignano, Proc. Combust. Inst. 18 (1980) 1365-1374.
- [19] J. W. Aldred, J. C Patel, A. Williams, Combust. Flame. 17 (2) (1971) 139-148.
- [20] A. J Marchese, F. L. Dryer, Combust. Flame. 105 (1996) 104-122.
- [21] C. K. Law, H. K. Law, AIAA Journal. 20 (4) (1982) 522-527.
- [22] B. D. Shaw, Combust. Flame. 81 (1990) 277-288.
- [23] N.W. Sorbo, C. K. Law, D. P. Y. Chang and R. R. Steeper, Proc. Combust. Inst. 22 (1989) 2019.
- [24] T. Kadota, H. Hiroyasu, Proc. Combust. Inst. 18 (1981) 275-282.
- [25] J. P. Delplanque, W. A. Sirignano, Int. J. Heat Mass Transfer. 36 (1993) 303-314.
- [26] G. Zhu, S. K. Aggarwal, Int. J. Heat Mass Transfer. 43 (2000) 1157-1171.
- [27] M. K. Jain, *Solution of Differential Equations*, Second Edition, Wiley-Eastern Limited, 1984.
- [28] O. L. Gülder, Transac. of the ASME, 108 (1986) 376-380.
- [29] R. C. Reid, J. M. Prausnitz, B. E. Poling, *The Properties of Gases and Liquids*, Fourth Edition, McGraw Hill Book Company, 1989.
- [30] G. L. Hubbard, V. E. Denny, A. F. Mills, Int. J. Heat Mass Transfer, 18 (1975) 1003-1008.
- [31] S. R. Turns, *An Introduction to Combustion Concepts and Applications*, McGraw Hill International Edition, 1996.
- [32] C. K. Law, W. A. Sirignano, Combust. Flame. 28 (1977) 175-186.
- [33] G. L. Borman, K. W. Ragland, *Combustion Engineering*, McGraw-Hill International Editions, 1998.

APPENDIX A

**Table A.1: Constants for Evaluating Flame Temperature by
 Gülder's Method [28]**

<i>Constants</i>	$0.3 \leq \phi \leq 1.0$		$1.0 < \phi \leq 1.6$	
	$0.92 \leq \theta < 2$	$2 \leq \theta \leq 3.2$	$0.92 \leq \theta < 2$	$2 \leq \theta \leq 3.2$
<i>A</i>	2361.7644	2315.7520	916.8261	1246.1778
<i>α</i>	0.1157	-0.0493	0.2885	0.3819
<i>β</i>	-0.9489	-1.1141	0.1456	0.3479
<i>λ</i>	-1.0976	-1.1807	-3.2771	-2.0365
<i>a</i> ₁	0.0143	0.0106	0.0311	0.0361
<i>b</i> ₁	-0.0553	-0.0450	-0.0780	-0.0850
<i>c</i> ₁	0.0526	0.0482	0.0497	0.0517
<i>a</i> ₂	0.3955	0.5688	0.0254	0.0097
<i>b</i> ₂	-0.4417	-0.5500	0.2602	0.5020
<i>c</i> ₂	0.1410	0.1319	-0.1318	-0.2471
<i>a</i> ₃	0.0052	0.0108	0.0042	0.0170
<i>b</i> ₃	-0.1289	-0.1291	-0.1781	-0.1894
<i>c</i> ₃	0.0827	0.0848	0.0980	0.1037